BAROCLINIC WAVES IN CLIMATES OF THE EARTH'S PAST

A.B.G. BUSH
Dept. of Earth and Atmospheric Sciences
University of Alberta
Edmonton, Alberta, Canada
andrew.bush@ualberta.ca

Apologies for some of the figures in this version; if you need better quality ones please send me an email. Please reference as follows:

Bush, A.B.G., 2003: Baroclinic waves in Climates of the Earth's past. In "Nonlinear Processes in Geophysical Fluid Dynamics". O.U. Velasco-Fuentes, J. Sheinbaum and J.L. Ochoa de la Torre (Eds.). Kluwer Academic Publishers. Dordrecht, The Netherlands. in press.

Abstract.

Our understanding of the climates that have existed on Earth through its history has increased tremendously through a combination of geophysical fluid dynamics, geological evidence, and numerical modelling. Evolution of our Earth's orbit redistributes incoming solar radiation latitudinally and temporally and is believed to have been responsible for changing the strength of the south Asian monsoon, expanding and contracting desert regions, and perhaps even initiating the (geologically) recent cycles of glaciation. Evolution of the atmosphere itself, in terms of the amount of atmospheric greenhouse gases in it, affects the amount of water vapour in the atmosphere, global temperatures, and meridional temperature gradients. Topographic forcing by the massive continental ice sheets that have existed in the past is believed to have significantly altered the jet stream circulation.

All of these factors–the distribution of incoming solar radiation, atmospheric greenhouse gases, and topograhic forcing–affect the mean baroclinic structure of our atmosphere, the amount of baroclinic wave activity present, and the eddy heat and momentum fluxes associated with these eddies. The equatorward flux of easterly momentum during the barotropic decay phase of these waves, in particular, plays a key role in determining the strength of upper level convergence and subsidence in the subtropics and, hence, the low-level meridional pressure gradient that helps to maintain the tropical trade winds. Through a series of numerical experiments with a coupled atmosphere-ocean general circulation model, it is shown that all of the factors listed above have played a role in determining the amount of baroclinic wave activity in climates of the Earth's past and that changes in tropical circulations are consistent with the notion that the baroclinic eddy field plays an important role in determining the mean state in the tropics.

1. Introduction

Maintenance of the atmospheric and oceanic general circulations involves a complex balance between boundary condition forcing (e.g., bottom topography and incoming solar radiation) and the nonlinear dynamical processes that occur within each medium (e.g., baroclinic eddies and convection, to name only two). The relative roles of the dynamical processes in producing the mean atmospheric general circulation that we observe today has received much attention (e.g., Held and Hou, 1980; Pfeffer, 1981; Lindzen and Hou, 1988; Haynes and Shepherd, 1989; Chang, 1996; Becker *et al.*, 1997; Kim and Lee, 2001a,b). While the role of midlatitude baroclinic eddies in fully generating and sustaining the Ferrel cell has been established (e.g., Held and Hou, 1980), their role in governing observed mean tropical circulations such as the Hadley cell is more debatable. It was at first believed that their contribution is small and that diabatic heating from tropical convection was the primary driving force for the Hadley circulation (e.g., Pfeffer, 1981). More recently, however, the relative role of eddies in driving the Hadley circulation has been shown to be much larger (approximately 75%) when the feedback between eddy momentum flux, surface friction, and tropical moisture convergence is taken into account in the computation of direct diabatic forcing (Kim and Lee, 2001a,b).

Changes in mean wind strength in the tropics are extremely important in a coupled atmosphere-ocean system because of positive dynamical feedbacks [e.g., Philander, 1985; Xie, 1998]. The tropical oceans are quite sensitive to changes in Hadley cell strength because, through angular momentum conservation, an increase in Hadley cell strength implies stronger surface easterlies which, in turn, produce stronger oceanic upwelling and colder sea surface temperatures (SSTs) through the feedbacks that are responsible for the El Niño Southern Oscillation (e.g., Philander, 1990). Therefore, midlatitude baroclinic eddies are likely to contribute, at least in part, to the generation of the mean state of the tropical oceans.

Some aspects of our climate's past may provide insight into this hypothesis because our atmosphere-ocean system has evolved through many states quite different than the one in which it is presently found and, moreover, geological proxy data exist and give clues as to what climatic conditions existed in the past.

For example, repeated glaciations over the past 900,000 years have dramatically altered surface topography by imposing massive Northern Hemisphere ice sheets up to 3 kilometers thick (e.g., Peltier, 1994) that reflect much of the incoming solar radiation and alter the path of the Northern Hemisphere jet stream (Bush and Philander, 1999; Hall *et al.*, 1996). Geological evidence, as inferred from aeolian deposits (e.g., Sarnthein *et al.*, 1981; Farrell *et al.*, 1995), productivity estimates (Pedersen, 1983; Lyle *et al.*, 1992), grain size analysis (Rutter, 1992), and planktonic foraminifera (Andreasen and Ravelo, 1997), suggest that the mean atmospheric circulation was stronger during these glacial periods.

Conversely, during equable climates when atmospheric carbon dioxide was higher than it is today, such as the Cretaceous (Berner, 1991), high latitude surface temperatures were much warmer and hence, through thermal wind balance, weaker westerlies and a weaker general circulation have been proposed (e.g., Barron and Washington, 1982; Sloan and Barron, 1990).

During periods such as the early-mid Holocene (∼10,000-5,000 years before present) when the seasonal and latitudinal distribution of incoming solar radiation favoured a much more seasonal climate in the Northern Hemisphere, atmospheric winds were different, particulary those of the south Asian monsoon (e.g., Wright *et al.*, 1993; Prell, 1984; Clemens and Prell, 1990; Prell and Kutzbach, 1992).

Baroclinic instability of the atmosphere's jet streams is highly dependent on the shears present in the climatological mean state. The factors listed above (i.e., solar forcing, topographic forcing, and the amount of carbon dioxide present in the atmosphere) all have the potential to alter the mean state of the atmosphere and hence the strength and frequency of baroclinic eddies. Are the changes that would be produced in the tropics by changing these factors consistent with the notion that baroclinic eddies play an important role in governing tropical circulations?

This question is addressed through analysis of a series of numerical experiments performed with the coupled atmosphere-ocean general circulation model developed at the Geophysical Fluid Dynamics Laboratory in Princeton, NJ. The results of Bush (2001) are extended here to include analyses of four experiments that explore a broader range of boundary conditions that have occured in Earth's past. First, a simulation of the Last

Glacial Maximum (~21,000 years B.P.) is analyzed to determine the effect of massive ice sheets on the circulation. Second, a simulation of the mid-Holocene (~6,000 years B.P.) is analyzed to determine the effect of an increased seasonal cycle in the Northern Hemisphere. Third, a simulation with double the amount of atmospheric carbon dioxide is analyzed to determine the effect of high latitude warming on baroclinic wave activity and the general circulation. Fourth, a simulation in which the Earth is completely ice-covered, as has been proposed for the Neoproterozoic (~600-800 million years before present; Hoffman *et al.*, 1998; Hyde *et al.*, 2000), is analyzed to determine the impact of rendering surface baroclinicity negligible. While the nature of the Snowball Earth is a matter of some debate (the debate is centred on whether or not the tropical oceans were completely ice-covered or whether open water refugia existed), it is assumed here that the oceans were completely ice-covered; therefore, this simulation is performed with the atmosphere-only model only. Numerical results are included here to provide an example of the dynamics that may have occured during one of the most extreme climates of Earth's past. Results of these four experiments are compared to a control simulation for today's climate.

A brief description of the coupled model is given in the next section, followed by the results and discussion in section 3 and concluding remarks in section 4.

2. Configurations of the model

For brevity, the reader is referred to Bush and Philander (1999) for full details of the numerical model and for a description of the model configuration in the LGM simulation. Key points are that: the atmospheric model (Gordon and Stern, 1982) is spectral with rhomboidal 30 truncation and a 216 second time step; the oceanic model (MOM, version 2; Pacanowski *et al.*, 1991) uses finite-differencing with a resolution of 2.25^o in latitude, 3.75^o in longitude, 15 vertical levels, and a 1-hour time step, and; dynamic and thermodynamic coupling between the models is performed once per day of integration time. In the LGM simulation, continental ice sheets are imposed according to reconstructions (Peltier, 1994), sea level is lowered by 120 meters (Fairbanks, 1989), glacial land surface albedo is imposed (CLIMAP, 1981), and atmospheric carbon dioxide is set to 200 ppm.

The model configuration for the mid-Holocene simulation is identical to that of the control simulation with the exception that the orbital parameters of obliquity, eccentricity, and longitude of perihelion are set to those appropriate to 6,000 years B.P. (Berger, 1992). In particular, obliquity at 6,000 B.P. was 24.1^o as opposed to the modern 23.446^o so an increased seasonal cycle is expected. Also, perihelion occured during boreal summertime (today it occurs in austral summertime). The increased CO_2 simulation is identical to the control simulation except that the amount of atmospheric carbon dioxide is doubled. The Snowball simulation assumes flat continental ice over the continents (which are all located in the tropics; see Hyde *et al.*, 1990) and sea ice over all of the oceans; bare surface albedo is therefore set to 0.6 everywhere in the tropics and increases to 0.8 at the poles. A 7% reduction in solar luminosity is assumed, as appropriate for the early Neoproterozoic (Endal and Sofia, 1981).

The coupled simulations are decadal in timescale (specifically, 70 years for the control and CO_2 simulations and 25 years for the others). The simulations are sufficiently long for the atmosphere and the upper ocean to have reached a new radiative equilibrium state and for the oceanic wind-driven circulation to be established. Any possible influence of benthic ocean currents on SST are therefore neglected in these simulations. Model output fields are averaged to produce monthly mean data, from which the following results were obtained. In the discussion to follow we will focus on changes in eddy activity in the Northern hemisphere since this is where most of the changes occur from, for example, topographic forcing in the LGM simulation and radiative forcing in the mid-Holocene simulation. Changes in the Southern hemisphere eddies are small in comparison.

3. Simulated mean climates and baroclinicity

There is a relatively wide range of baroclinicities in the climatological mean state of these simulations (Figure 1a) with the greatest existing in the LGM simulation (when large ice sheets cool the Northern Hemisphere polar latitudes) and the smallest in the Snowball simulation (when the planet is completely ice-covered).

In the Northern Hemisphere winter (Figure 1b), baroclinicity increases above its climatological value by 30% in the control simulation and by 34% in the mid-Holocene simulation. Winter values are therefore greater than today in the LGM and mid-Holocene simulations and are lesser than today in the CO2 and Snowball simulations.

Since baroclinic eddies develop primarily in wintertime, these differences in mean wintertime baroclinicity should also be reflected in the Northern Hemisphere momentum flux. The total northward momentum transport is $[\overline{VU}]$, where a bar denotes a time average and square brackets denote a zonal average. The following decomposition then follows (e.g., Peixoto and Oort, 1992):

$$[\overline{VU}] = [\overline{V}][\overline{U}] + [\overline{V'U'}] + [\overline{V^*U^*}]. \tag{1}$$

where a prime indicates a departure from the time mean and a star indicates a departure from the zonal mean. Terms on the right hand side therefore

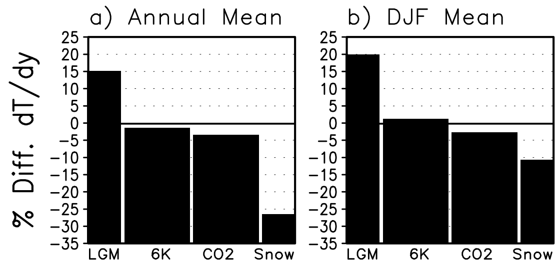

Figure 1. **a)** Climatological, zonally averaged, surface baroclinicities averaged between 30-60N, shown as a percentage difference from the control simulation (the value for which is -0.5^o per degree of latitude) for the Last Glacial Maximum (LGM) the mid-Holocene (6K), the increased CO_2 (CO2) and the Snowball (Snow) simulations. **b)** Same as in **a)** but for the December-January-February means (the value in the control simulation is -0.65^o per degree of latitude).

represent contributions to the total momentum flux from, respectively, the mean meridional circulation, the transient eddies, and the stationary eddies. Note that because monthly mean values are used in these diagnostics, all interannual variability is included in the stationary eddy statistics (see Peixoto and Oort (1992)). Although we wish to focus here only on changes in the climatological mean states in the simulations, we note that there are also changes in interannual variability in the three coupled model experiments (the LGM, mid-Holocene, and increased CO_2 simulations). Some differences in the stationary eddy statistics may therefore be attributable to these changes.

The net momentum transport in all simulations (Figure 2) indicates that the LGM and mid-Holocene simulations have greater equatorward flux of easterly momentum than the control, while the CO2 and Snowball simulations have smaller fluxes. A breakdown of the contributions in the LGM and mid-Holocene simulations indicates that it is the stationary eddies that contribute most to the increased flux in the LGM simulation (although transient eddy activity also increases), whereas it is the transient eddies that contribute most to the increase in the mid-Holocene simulation (Figures 2b-c). Additional high latitude momentum fluxes in the LGM simulation are related to splitting of the midlatitude jet by the Cordilleran and Laurentide ice sheets over North America.

Contributions of midlatitude eddies to both heat and momentum transport are readily visualized by the E-P flux vectors, whose positive horizontal and vertical components, F_λ and F_p, represent, respectively, equatorward flux of westerly momentum and poleward heat transport. They may be

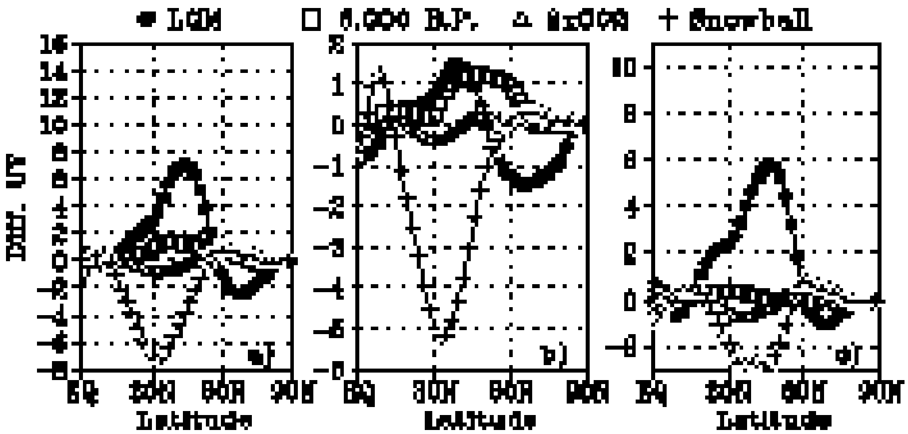

Figure 2. Changes (experiment minus control) in northward momentum transport in the Northern hemisphere by **a)** all motions, **b)** transient eddies, and **c)** stationary eddies. Units are m^2/s^2. Note that the axis scale is different between the three panels. (Peak values in the control simulation are 7.3, 5, and 3.1, respectively.)

written as (e.g., Piexoto and Oort, 1992):

$$F_\lambda = -\frac{2\pi R^2 \cos^2(\phi)}{g} \quad [U^* V^*],$$

$$F_p = \frac{2\pi R^3 \cos^2(\phi)}{g} \quad f[V^*\Theta^*](\partial\Theta_s/\partial p)^{-1}. \tag{2}$$

Here, R is the Earth's radius, g is gravity, f is the Coriolis parameter, ϕ is latitude, Θ is potential temperature and Θ_s is the global mean potential temperature on a pressure surface.

In the control simulation, the baroclinic eddy field generates E-P flux vectors that indicate poleward heat transport in the lower-mid troposphere, with equatorward flux of easterly momentum in the upper troposphere (Figure 3a). The values plotted are annual means, so the entire life cycles of all eddies (i.e., their baroclinic growth, F_p and their barotropic decay, F_λ) is included (e.g., Simmons and Hoskins, 1980; Edmon *et al.*, 1980). Differences between the simulations and the control (Figures 3b-d) indicate greater momentum flux in the LGM and mid-Holocene simulations, and less in the CO2 simulation. E-P fluxes in the Snowball simulation are extremely small and are therefore not shown in this figure. In the LGM simulation, the northern hemisphere jet stream is split north and south by the Laurentian ice sheet over North America and exhibits greater baroclinicity downstream

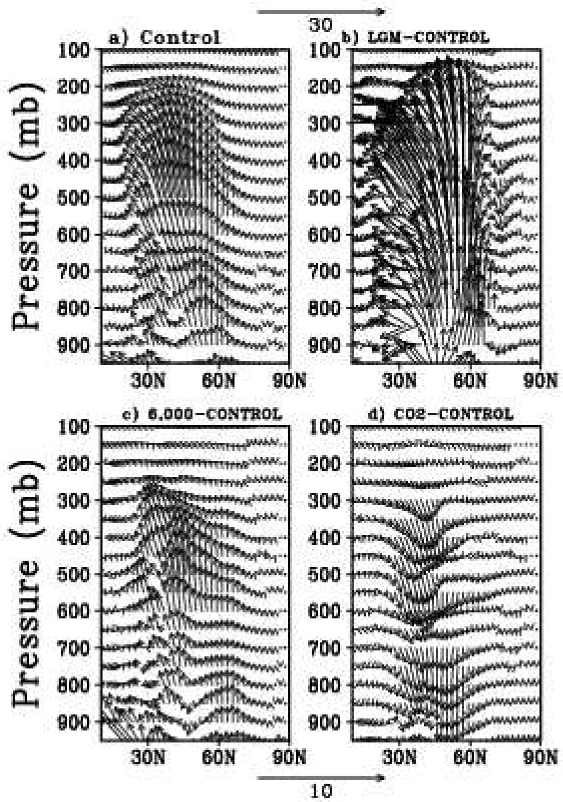

Figure 3. **a)** E-P flux vectors (as defined in the text) in the control simulation, from transient and stationary eddies. Differences in E-P flux are shown for **b)** the LGM, **c)** the mid-Holocene, and **d)** CO2. Vector components have been scaled down by the common factor $\frac{2\pi R^2}{g}$, so that the units are m^2/s^2. The arrow scale for panels **a)** and **b)** is shown above the figure, whereas the scale for panels **c)** and **d)** is shown below the figure.

of the ice sheet in the Atlantic storm track (e.g., Hall *et al.*, 1996; Bush and Philander, 1999). Analysis of the separate contributions by transient and stationary eddies (not shown) indicates that stationary eddies dominate in the LGM simulation, whereas transient eddies contribute more in the mid-Holocene simulation. In the increased CO_2 simulation, the contributions from each are comparable.

In the control simulation the greatest convergence of momentum flux is in the upper troposphere of the subtropics on the poleward edge of the tropical Hadley cell (c.f. Fig. 3a). Increased convergence in this region in the LGM and mid-Holocene simulations increases subtropical subsidence, whereas decreased convergence in the CO2 and Snowball simu-

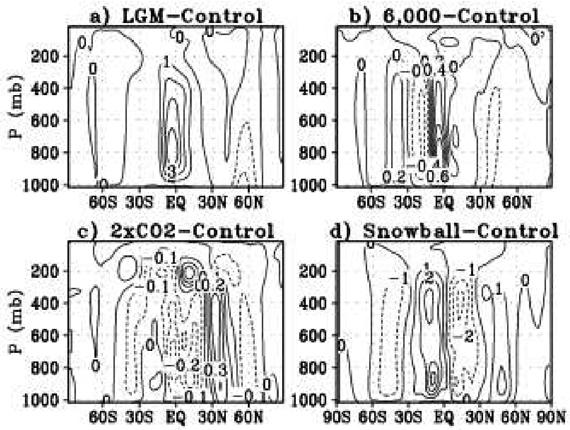

Figure 4. Differences (experiment minus control) in the annual mean Hadley circulation for **a)** the LGM simulation, **b)** the mid-Holocene simulation, **c)** the increased CO_2 simulation, and **d)** the Snowball simulation. The sign convention is such that positive values indicate a clockwise circulation in the plane of the diagram. Units are 10^{10}kg/s.

lations decreases subsidence. Differences in the zonal mean Hadley circulation do show such changes (Figure 4) with magnitudes that are in agreement with the differences in momentum transport (c.f. Fig. 2), in the sense that the LGM simulation shows the strongest increase in subsidence, the mid-Holocene simulation a lesser increase, the increased CO_2 simulation a decrease, and the Snowball simulation a large decrease. For reference, the Hadley cells in the control simulation have maximum amplitudes of -6.1×10^{10} kg/s and 5×10^{10} kg/s in the Southern and Northern hemispheres, respectively. The Ferrel cells have maximum amplitudes of 2.4×10^{10} kg/s and -2.6×10^{10} kg/s in the Southern and Northern hemispheres, respectively.

The meridional pressure gradient between the near tropics and the subtropics is, climatologically, in near geostrophic balance with the zonal wind field. That is, the higher surface pressure of the subtropics, caused by subsidence of the air between the Hadley and Ferrel cells, creates a positive meridional pressure gradient that balances the mean easterly trade winds. [For climatological mean fields, geostrophy holds quite well close to the equator, to within 5 degrees of latitude.] Without any compensating changes in equatorial pressure, these changes in subtropical subsidence should therefore alter the strength of the equatorial easterlies. Since topographic heights have been altered in two experiments (LGM and Snowball), there are concomitant changes in surface pressures. Between the control, mid-Holocene, and increased CO_2 simulations there is a change of less than one millibar in the mean equatorial pressure. In the LGM and Snowball

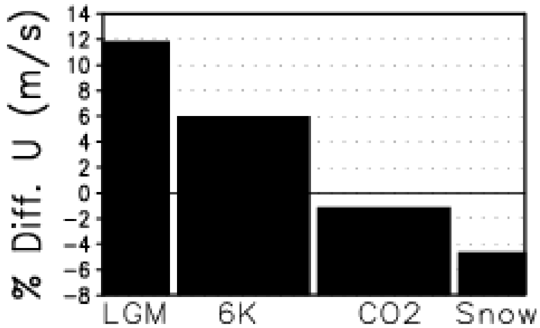

Figure 5. Climatological, zonally averaged, surface zonal wind speed change between 10S and 10N, shown as a percentage difference from the control simulation (the value for which is −4.7 m/s).

simulations, however, equatorial pressures are 9 millibars higher and 17 millibars lower, respectively, because of the increased and decreased topographic heights. It is assumed that these changes are uniform spatially so that the gradients are not affected by this mechanism.

Simulated changes in mean zonal wind speed in the tropics are in agreement with what would be inferred from the changes in subtropical subsidence (Figure 5; note that a positive change in zonal wind speed implies stronger trade easterlies). The change in LGM zonal winds is the greatest of all the simulations, despite the fact that the greatest change in momentum transport is in the Snowball simulation. However, in the LGM, mid-Holocene, and increased CO_2 simulations the oceans are allowed to respond to changes in wind speed. There is, therefore, an element of atmosphere-ocean feedback in these simulations that is precluded in the Snowball simulation. Increased zonal wind speeds in the LGM and mid-Holocene simulations increase oceanic upwelling, particularly in the eastern tropical Pacific. This upwelling increases the extent of the Pacific cold tongue which, in turn, increases the zonal pressure gradient along the equator. This amplifies the winds even further, in the type of positive feedback that controls the El Niño Southern Oscillation, leading to a more La Niña-like climatological mean state. In the increased CO_2 simulation, the opposite holds true, and decreased easterlies reduce equatorial upwelling and lead to a more El Niño-like mean state.

The east-west tilt of the mean thermocline in the tropical Pacific therefore increases in the LGM and mid-Holocene simulations, and is smaller in the increased CO_2 simulation (Figure 6). This result is consistent with the changes in mean zonal wind speeds, and has implications for the frequency of interannual variability (Fedorov and Philander, 2000).

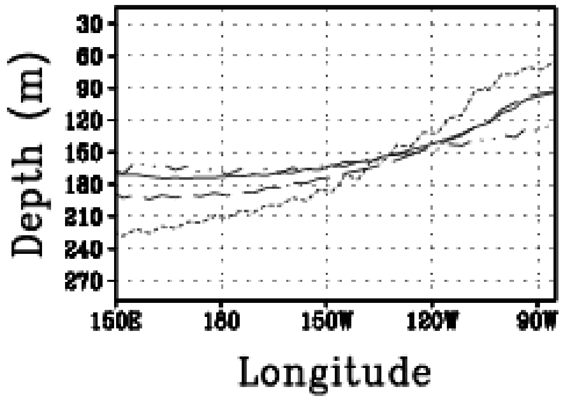

Figure 6. Depth of the 18^{o}C isotherm in the Pacific Ocean in the coupled model simulations. **Solid line:** control simulation; **short dashed line:** LGM simulation; **long dashed line:** mid-Holocene simulation; **dashed-dot-dot line:** increased CO_2 simulation.

4. Conclusions

Simulated changes in the mean state of the tropical Pacific Ocean are consistent with the idea that, through the momentum fluxes associated with their decay phase, midlatitude baroclinic eddies play a role in governing the strength of subtropical convergence in the upper troposphere, subsidence, surface pressure gradients, and hence equatorial trade winds. Moreover, the changes in eddy activity are consistent with the changes in mean state baroclinicity and topographic forcing that are prescribed in each simulation. Atmosphere-ocean interactions in the tropics act to amplify the response beyond what would be expected from the change in momentum flux alone. While evidence exists for stronger trade winds and a steeper thermocline tilt at the LGM, proxy data have yet to be provided for other times such as the mid-Holocene.

References

Andreasen, D., and A. C. Ravelo, Tropical Pacific Ocean thermocline depth reconstructions for the Last Glacial, *Paleoceanography*, 12, 395-414, 1997.

Barron, E.J., and W. Washington, The atmospheric circulation during warm, geologic periods: Is the equator-to-pole surface temperature gradient the controlling factor? *Geology*, 10, 633-636, 1982.

Becker, E., G. Schmitz, and R. Geprags, The feedback of midlatitude waves onto the Hadley cell in a simple general circulation model. *Tellus*, 49A, 182-199, 1997.

Berger, A., Orbital variations and insolation database, IGBP PAGES/World Data Center-A for Paleoclimatology Data Contribution Series # 92-007. NOAA/N GDC Paleoclimatology Program, Boulder CO, USA.

Berner, R.A., A model for atmospheric CO_2 over Phanerozoic time, *Am. J. Sci.*, 291, 339-376, 1991.

Bush, A.B.G., Assessing the impact of mid-Holocene insolation on the atmosphere-ocean system. *Geophy. Res. Lett.*, 26, 99-102, 1999.

Bush, A.B.G., Simulating climates of the Last Glacial Maximum and of the mid-Holocene: Wind changes, atmosphere-ocean interactions, and the tropical thermocline. *AGU Monograph Series 126 (The Oceans and Rapid Climate Change: Past, Present, and Future)*, 135-144, 2001.

Bush, A.B.G. and S.G.H. Philander, The climate of the Last Glacial Maximum: Results from a coupled atmosphere-ocean general circulation model. *J. Geophys. Res.*, 104, 24,509-24,525, 1999.

Chang, E.K.M., Mean meridional circulation driven by eddy forcings of different time scales. *J. Atmos. Sci.*, 53, 113-125, 1996.

Clemens, S.C. and W.L. Prell, Late Pleistocene variability of Arabian Sea summer-monsoon winds and dust source-area aridity: A record from the lithogenic component of deep-sea sediments, . *Paleoceanogr.*, **5**, 109-145, 1990.

Climate: Long-Range Investigation, Mapping, and Prediction (CLIMAP) Project Members, Seasonal reconstructions of the Earth's surface at the last glacial maximum, *Map and Chart Series MC-36*, Geol. Soc. of Am., Boulder, CO, 1981.

Edmon, H.J., B.J. Hoskins, and M.E. McIntyre, Eliassen-Palm cross-sections for the troposphere, *J. Atmos. Sci.*, 37, 2600-2616, 1980.

Endal, A.S. and S. Sofia, Rotation in solar-type stars, I, Evolutionary models for the spindown of the sun. *Astrophys. Jour.*, 243, 625-640, 1981.

Fairbanks, R.G., A 17,000-year glacio-eustatic sea level record: Influence of glacial melting rates on Younger Dryas event and deep-ocean circulation, *Nature*, 342, 637-642, 1989.

Fedorov, A.V. and S.G.H. Philander, Is El Niño Changing? *Science*, 288, 1997-2002, 2000.

Gordon, C.T., and W. Stern, A description of the GFDL global spectral model, *Mon. Weather Rev.*, 110, 625-644, 1982.

Hall, N.M.J., P.J. Valdes, and B. Dong, The maintenance of the last great ice sheets: A UGAMP GCM study, *J. Clim.*, 9, 1004-1019, 1996.

Haynes, P.H., and T.G. Shepherd, The importance of surface pressure changes in the response of the atmosphere to zonally-symmetric thermal and mechanical forcing, *Q. J. R. Meteorol. Sci.*, 115, 1181-1208, 1989.

Held, I.M., and A.Y. Hou, Nonlinear axially symmetric circulations in a nearly inviscid atmosphere, *J. Atmos. Sci.*, 37, 515-533, 1980.

Hoffman, P.F., A.J. Kaufman, G.P. Halverson, and D.P. Schrag, A Neoproterozoic snowball earth, *Science*, 281, 1342-1346, 1998.

Hyde, W.T., T.J. Crowley, S.K. Baum, and W.R. Peltier, Neoproterozoic 'snowball Earth' simulations with a coupled climate/ice-sheet model, *Nature*, 405, 425-429, 2000.

Kim, H.K., and S. Lee, Hadley cell dynamics in a primitive equation model: Part I. Axisymmetric flow. *J. Atmos. Sci.*, 58, 2845-2858, 2001.

Kim, H.K., and S. Lee, Hadley cell dynamics in a primitive equation model: Part II. Nonaxisymmetric flow. *J. Atmos. Sci.*, 58, 2859-2871, 2001.

Kutzbach, J.E. and B.L. Otto-Bliesner (1982). The sensitivity of the African-Asian monsoonal climate to orbital parameter changes for 9000 years B.P. in a low-resolution general circulation model. *J. Atmos. Sci.*, 39, 1177-1188.

Lindzen, R.S., and A.Y. Hou, Hadley circulations for zonally averaged heating off the equator, *J. Atmos. Sci.*, 45, 2416-2427, 1988.

Lyle, M.W., F.G. Prahl, M.A. Sparrow, Upwelling and productivity changes inferred from a temperature record in the central equatorial Pacific, *Nature*, 355, 812-815, 1992.

Otto-Bleisner, B.L., El Niño/La Niña and Sahel precipitation during the middle Holocene. *Geophys. Res. Lett.*, 26, 87-90, 1999.

Pacanowski, R.C., K. Dixon, and A. Rosati, *The GFDL Modular Ocean Model user guide, GFDL Ocean Group Tech. Rep. 2*, Geophys. Fluid Dyn. Lab., Princeton, N.J., 1991.

Pedersen, T.F., Increased productivity in the eastern equatorial Pacific during the last glacial maximum (19,000 to 14,000 yr B.P.), *Geology*, 11, 16-19, 1983.

Peixoto, J.P. and A.H. Oort, *Physics of Climate*, American Institute of Physics, New

York, 520 pp., 1992.
Peltier, W.R., Ice age paleotopography, *Science*, 265, 195-201, 1994.
Pfeffer, R.L., Wave-mean flow interactions in the atmosphere. *J. Atmos. Sci.*, 38, 1340-1359, 1981.
Philander, S.G.H., El Niño and La Niña, *J. Atmos. Sci.*, 42, 2652-2662, 1985.
Philander, S.G.H., *El Niño, La Niña, and the Southern Oscillation*, Academic Press, New York, 293 pp., 1990.
Prell, W.L., Monsoonal climate of the Arabian Sea during the late Quaternary: A response to changing solar radiation. *In* "Milankovitch and Climate" (A. Berger *et al.*, Eds.), pp. 349-366. Reidel, Dordrecht, 1984.
Prell, W.L. and J.E. Kutzbach, Sensitivity of the Indian monsoon to forcing parameters and implications for its evolution. *Nature, 360*, 647-652, 1992.
Rutter, N.W., Presidential Address, XIII INQUA Congress 1991: Chinese loess and global change, *Quat. Sci. Rev.*, 11, 275-281, 1992.
Sarnthein, M., G. Tetzlaff, B. Koopman, K. Wolter, and U. Pflaumann, Glacial and interglacial wind regimes over the eastern subtropical Atlantic and north-west Africa, *Nature*, 293, 193-196, 1981.
Simmons, A.J. and B.J. Hoskins, Barotropic influences on the growth and decay of non-linear baroclinic waves, *J. Atmos. Sci.*, 37, 1679-1684, 1980.
Sloan, L.C., and E.J. Barron, "Equable" climates during Earth history? *Geology*, 18, 489-492, 1990.
Wright, H.E. Jr., J.E. Kutzbach, T. Webb III, W.F. Ruddiman, F.A. Street-Perrott, and P.J. Bartlein (Eds.), "Global climates since the Last Glacial Maximum", 569 pp, University of Minnesota Press, Minneapolis, 1993.
Xie, S.-P., Ocean-atmosphere interaction in the making of the Walker circulation and the equatorial cold tongue, *J. Clim.*, 11, 189-201, 1998.